# Exponential Splitting for $n$-Dimensional Paraxial Helmholtz Equation with High Wavenumbers

Qin Sheng[†,1] and Hai-Wei Sun[‡,2]

[†] *Department of Mathematics and Center for Astrophysics, Space Physics and Engineering Research*
*Baylor University, One Bear Place, Waco, TX 76798-7328, USA*

[‡] *Department of Mathematics*
*University of Macau, Macao, China*

**Abstract**

This paper explores applications of the exponential splitting method for approximating highly oscillatory solutions of the $n$-dimensional paraxial Helmholtz equation. An eikonal transformation is introduced for oscillation-free platforms and matrix operator decompositions. It is found that the sequential, parallel and combined exponential splitting formulas possess not only anticipated algorithmic simplicity and efficiency, but also the accuracy and asymptotic stability required for highly oscillatory wave computations.

*Keywords:* exponential splitting, paraxial Helmholtz equation, high wavenumber, high oscillations, eikonal transformation, asymptotic stability

## 1. Introduction

Splitting strategies have been backbones of many highly straightforward yet accurate numerical methods for solving linear or nonlinear partial differential equations, in particular those oriented from important multiphysics applications or multiscale environments [1, 3, 5, 7]. In a splitting process, the underlying modeling equation is decomposed to several more durable subproblems

[1] Principal and corresponding author. Email address: Qin_Sheng@baylor.edu

[2] The second author is supported in part by research grants MYRG206(Y3-L4)-FST11-SHW from University of Macau and 005/2012/A1 from the FDCT of Macao.

to solve before a final approximation is obtained. A successful splitting procedure yields not only desirable accuracy, but also expected efficiency as well as stability in practical computations [2, 14].

Exponential splitting has been one of such strategies used frequently due to its extraordinary simplicity and capability in real applications. Let $\mathcal{D} \subset \mathbb{R}^n$ and $u \in \mathbb{C}$ be sufficiently smooth. Further, let $\mathcal{A}_1, \mathcal{A}_2, \ldots, \mathcal{A}_K$ be partial differential operators with smooth coefficients defined in a Banach space $\mathbb{H}$. Consider the differential equation

$$\frac{\partial u}{\partial z} = \sum_{k=1}^{K} \mathcal{A}_k u + f(u, z), \quad x \in \mathcal{D},\ z > z_0. \tag{1.1}$$

Assume that $\mathcal{D}_h$ is a mesh region superimposed on $\mathcal{D}$, and a suitable spatial discretization of (1.1) under proper boundary conditions yields the following semidiscretized system,

$$v' = \sum_{k=1}^{K} A_k v + g(v, z), \quad z > z_0, \tag{1.2}$$

where $A_1, A_2, \ldots, A_K \in \mathbb{C}^{s\times s}$ and $v,\ g \in \mathbb{C}^s$. Note that $A_1, A_2, \ldots, A_K$ do not, in general, commute. Let $A_1, A_2, \ldots, A_K$ be $z$-independent since otherwise an averaging coefficient method may be applied [8]. If $v(z_0) = v_0$ is an initial vector, and $\{z_0, z_1, z_2, \ldots, z_\ell, \ldots\}$ be a $z$-mesh for which $z_{\ell+1} - z_\ell = \tau > 0,\ \ell = 0, 1, 2, \ldots,$ are constructed through an adaptive mechanism [1, 6]. Then the solution of (1.2) can be expressed as

$$\begin{aligned} v(z_{\ell+1}) &= \exp\left\{\tau \sum_{k=1}^{K} A_k\right\} v(z_\ell) + \int_0^\tau \exp\left\{(\tau - \xi) \sum_{k=1}^{K} A_k\right\} \\ &\quad \times g(v(z_\ell + \xi), z_\ell + \xi) d\xi, \quad \ell = 0, 1, 2, \ldots \end{aligned} \tag{1.3}$$

An application of the trapezoid rule for the integral above leads to

$$v^{\ell+1} = \exp\left\{\tau \sum_{k=1}^{K} A_k\right\} \left(v^\ell + \frac{\tau}{2} g^\ell\right) + \frac{\tau}{2} g^{\ell+1},\ \ell = 0, 1, 2, \ldots, \tag{1.4}$$

where $v^\alpha,\ g^\alpha$ are mesh functions approximating $v(z_\alpha),\ g(v^\alpha, z_\alpha)$, respectively, and $B = \exp\left\{\tau \sum_{k=1}^{K} A_k\right\}$ serves as the amplification matrix while the source term is frozen [14, 17].

Denote

$$S(A_1, A_2, \dots, A_K, \tau) = \prod_{k=1}^{K} \exp(\tau A_k), \quad A_1, A_2, \dots, A_K \in \mathbb{C}^{s\times s}, \ \tau \in \mathbb{R}. \quad (1.5)$$

Then a typical sequential exponential splitting for approximating (1.3) is

$$\begin{aligned} \xi_s^\ell &= S(A_K, A_{K-1}, \dots, A_1, \tau/2)\left(w^\ell + \frac{\tau}{2} g^\ell\right); \\ w^{\ell+1} &= S(A_1, A_2, \dots, A_K, \tau/2)\xi_s^\ell + \frac{\tau}{2} g^{\ell+1}, \quad \ell = 0, 1, 2, \dots, \end{aligned} \quad (1.6)$$

where $w^\alpha$, $g^\alpha$ are mesh functions for approximating $v(z_\alpha)$, $g(v^\alpha, z_\alpha)$, respectively [1, 6, 14]. Further, while a typical parallel exponential splitting is

$$\begin{aligned} \xi_p^\ell &= S(A_K, A_{K-1}, \dots, A_1, \tau)\left(w^\ell + \frac{\tau}{2} g^\ell\right); \\ \xi_q^\ell &= S(A_1, A_2, \dots, A_K, \tau)\left(w^\ell + \frac{\tau}{2} g^\ell\right); \\ w^{\ell+1} &= \frac{1}{2}\left(\xi_p^\ell + \xi_q^\ell\right) + \frac{\tau}{2} g^{\ell+1}, \quad \ell = 0, 1, 2, \dots, \end{aligned} \quad (1.7)$$

a combined exponential splitting can be expressed as

$$w^{\ell+1} = \frac{1}{4}\left[2S(A_1, A_2, \dots, A_K, \tau/2)\xi_s^\ell + \xi_p^\ell + \xi_q^\ell\right] + \frac{\tau}{2} g^{\ell+1}, \quad \ell = 0, 1, 2, \dots. \quad (1.8)$$

Approximations (1.6)–(1.8) are second order accurate (see Appendix). They are ideal in multiphysics and multiscale applications [4, 5, 14]. They provide more convenient accesses to the standard splitting formulation as well as alternative ways to investigate characteristic splitting properties, such as the stability, convergence and errors, via the baseline first order formula (1.5) [12, 13]. This may continue improving our understanding of exponential splitting methods and beyond as we can see in this short note.

The aim of this paper is to explore aforementioned simplified procedures for the split numerical solution of a highly oscillatory multidimensional problem that models electromagnetic wave propagations in the form of either paraboloidal waves or Gaussian beams within a narrow cone. The particular wave phenomena have been essential in astrophysics and space physics, especially in inflationary cosmology when nonlinear dispersion relations are concerned [4, 7, 19]. Our study is organized as follows. In the next section, an $n$-dimensional paraxial Helmholtz equation is presented and decomposed to a nonlinear system via the eikonal transformation. Block-tridiagonal systems are acquired after an application of appropriate Padé approximation of (1.5). Section 3 is devoted to detailed analysis of the asymptotic stability concerned. It is shown that the splitting procedures are unconditionally asymptotically stable. Remarks are given when variations of algorithmic settings are introduced. In Sections 4 and 5, an illustrative simulation example and brief conclusions are given. Finally, the order of accuracy of generalized splitting formulas (1.6)-(1.8) is investigated in Section 6. The $h$-weighted spectral norm is used in the stability analysis.

## 2. Eikonal Transformation Based Exponential Splitting

Let $E$ be an $n$-dimensional electric field function and $z$ be the propagation direction of a beam. Further, let $x = (x_1, x_2, \ldots, x_n)^\top$ be the transverse vector, $\mathcal{D} = \{x : \ a < x_k < b, \ k = 1, 2, \ldots, n\}$ be the transverse domain, $\partial\mathcal{D}$ be its boundary and $\bar{\mathcal{D}} = \mathcal{D} \cup \partial\mathcal{D}$. We have the paraxial Helmholtz equation [11, 18],

$$2\mathbf{i}\kappa_0 r_0 \frac{\partial E}{\partial z} = \sum_{k=1}^{n} \frac{\partial^2 E}{\partial x_k^2} + \kappa_0^2 \left[ r^2(x, z) - r_0^2 \right] E, \quad x \in \mathcal{D}, \ z > z_0, \tag{2.1}$$

where $\mathbf{i} = \sqrt{-1}$, $\kappa_0$ is the wavenumber in free space, $r_0$ is the reference refractive index and $r(x, z)$ is the cross section index profile. Equation (2.1) models the propagation of a Gaussian beam in the $n$-dimensional field, or the flow covariance in quantum gravity around Lifshitz points [6, 7]. Lower dimensional versions of (2.1) have also played an important role in laser propagation modeling and laser-material interaction simulations [11]. Numerous numerical methods, including ADI, LOD and spectral schemes [3, 14, 16], have been designed and tested for solving (2.1). Many of them offer satisfactory approximations unless in cases where extra high wave parameters are utilized. It is evident that, when $\kappa_0 \gg 10$, the field function $E$ becomes highly oscillatory and continuing refinements of the computational mesh over $\mathcal{D}$ are required for maintaining acceptable computational accuracy [16]. This may not only lead to unrealistically small step sizes, but also impair the overall computational efficiency even when standard exponential splitting procedures are deployed [5, 15, 18]. It has been therefore meaningful to improve conventionally used exponential splitting strategies for overcoming above-mentioned difficulties.

To this end, let $\phi(x,z),\ \psi(x,z)$ be sufficiently smooth, $|\phi| \geq \phi_0 > 0$, and

$$|\phi_z| \ll \kappa|\phi|,\ \ |\phi_{zz}| \ll \kappa^2\,|\phi|\,,\quad x \in \mathcal{D},\ z > z_0,$$

where $\kappa = \kappa_0 r_0 \gg 1$ [16]. Consider the eikonal transform [11, 15],

$$E(x,z) = \phi(x,z)e^{\mathbf{i}\kappa\psi(x,z)},\quad x \in \mathcal{D},\ z > z_0.$$

A substitution of the above into (2.1) yields the following nonlinear differential system,

$$w_z = P\sum_{k=1}^{n} w_{x_k x_k} + f,\quad x \in \mathcal{D},\ z > z_0. \tag{2.2}$$

where

$$w = \left[\begin{array}{c}\phi\\ \psi\end{array}\right],\ \ P = \left[\begin{array}{cc}0 & \alpha\\ \beta & 0\end{array}\right], f = \left[\begin{array}{c}f_1\\ f_2\end{array}\right]$$

and

$$\alpha = \frac{\phi}{2},\ \beta = -\frac{1}{2\kappa^2\phi},\ f_1 = \sum_{k=1}^{n}\phi_{x_k}\psi_{x_k},\ f_2 = \frac{1}{2}\left(\sum_{k=1}^{n}\psi_{x_k}^2 - \frac{\kappa^2\left(r^2 - r_0^2\right)}{r_0^2}\right).$$

Further, we adopt the following initial and boundary conditions,

$$\begin{aligned} w(x,z) &= 0,\ x \in \partial\mathcal{D},\ z \geq z_0, & (2.3)\\ w(x,z_0) &= g_0(x),\ x \in \mathcal{D}, & (2.4)\end{aligned}$$

where $g_0$ is sufficiently smooth.

Note that the initial-boundary value problem (2.2)–(2.4) is oscillation-free even with high wavenumbers, mesh steps in numerical computations can thus be relatively large. This makes fast numerical solutions of (2.1) to be realistic. In fact, computational results from exponential splitting schemes or spectral approximations based on (2.2) have demonstrated its huge potential, though the study of its numerical stability is still in an infancy, partially due to relatively complex operator structures of (1.6)–(1.8) [6, 15, 16].

Given $m \gg 1$. For $h = (b-a)/(m+1)$ and $x_{k,0} = a,\ x_{k,m+1} = b,\ k = 1,2,\ldots,n$, we define a transverse mesh $\mathcal{D}_h = \{(x_{1,k_1}, x_{2,k_2}, \ldots, x_{n,k_n}) : x_{k,j} = x_{k,j-1} + h,\ j = 1,2,\ldots,m;\ k = 1,2,\ldots,n\}$. Denote $f_{k_1,k_2,\ldots,k_n}(z) = f(x_{1,k_1}, x_{2,k_2}, \ldots, x_{n,k_n}, z),\ x \in \mathcal{D}_h$. Approximating the second derivatives in (2.2) by central differences on $\mathcal{D}_h$ and utilizing (2.3), we acquire the following semidiscretized system of $(2m)^n$ equations,

$$w' = \sum_{k=1}^{n} A_k w + f, \tag{2.5}$$

together with (2.4), where

$$A_k = \frac{1}{h^2}\Big(\overbrace{I_{2m} \otimes \cdots \otimes I_{2m}}^{n-k}\Big) \otimes T \otimes I_2 \otimes \Big(\overbrace{I_{2m} \otimes \cdots \otimes I_{2m}}^{k-1}\Big) D, \quad k = 1, \ldots, n,$$

in which $\otimes$ stands for the Kronecker product, $I_\alpha$ is the $\alpha \times \alpha$ identity matrix,

$$T \;=\; \begin{bmatrix} -2 & 1 & & & \\ 1 & -2 & 1 & & \\ & \ddots & \ddots & \ddots & \\ & & 1 & -2 & 1 \\ & & & 1 & -2 \end{bmatrix} \in \mathbb{R}^{m \times m},$$

and

$$D = \operatorname{diag}\left(P_{k_1,k_2,\ldots,k_n}\right), \; w = \left(w_{k_1,k_2,\ldots,k_n}^{\top}\right)^{\top}, \; f = \left(f_{k_1,k_2,\ldots,k_n}^{\top}\right)^{\top}.$$

The notation $\chi_{k_1,k_2,\ldots,k_n}$ used above means that the components range from $\chi_{1,1,1,\ldots,1}$ to $\chi_{m,m,m,\ldots,m}$ in the fashion that

1. for each set of indexes $k_2, \ldots, k_n$, values of $k_1$ increase from 1 to $m$ monotonically;
2. for indexes $k_2, \ldots, k_n$, those on the left has priorities to increase from 1 to $m$ monotonically first.

Apparently, $T$ is Toeplitz, symmetric and tridiagonal and (2.5) carries a local truncation error of the size $\mathcal{O}(h^2)$. Consider the spectral norm. We have

**Lemma 2.1.**

$$\|D\|_2 = \frac{1}{2\kappa}, \; \|T\|_2 = 4 \max_{1 \le k \le m} \sin^2 \frac{k\pi}{m+1}.$$

*Proof.* It is observed that

$$P_{k_1,k_2,\ldots,k_n} P^{\top}_{k_1,k_2,\ldots,k_n} = \begin{bmatrix} \alpha_{k_1,k_2,\ldots,k_n}\beta_{k_1,k_2,\ldots,k_n} & 0 \\ 0 & \alpha_{k_1,k_2,\ldots,k_n}\beta_{k_1,k_2,\ldots,k_n} \end{bmatrix}.$$

Thus,

$$\|P_{k_1,k_2,\ldots,k_n}\|_2 = \sqrt{\alpha_{k_1,k_2,\ldots,k_n}\beta_{k_1,k_2,\ldots,k_n}} = \sqrt{\frac{1}{4\kappa^2}} = \frac{1}{2\kappa}.$$

Therefore the first equality is true. Proofs of the second equality is conventional and can be found in existing discussions including [8, 16]. □

Now, with $A_k,\ k = 1, 2, \ldots, n$, frozen at $z_\ell$ and the truncation error dropped, the numerical solution of (2.5) can be computed via any of second order splitting (1.6)–(1.8). However, due to the participation of (1.5), we only need to focus at the following building block formula for the analysis of numerical stability.

$$y^{\ell+1} = S(A_1, A_2, \ldots, A_n, \tau)\left(y^\ell + \frac{\tau}{2}g^\ell\right) + \frac{\tau}{2}g^{\ell+1},\ \ell = 0, 1, 2, \ldots$$

Replace the matrix exponentials in $S$ by [1/1] Padé approximants, respectively. We obtain readily our baseline implicit decomposition scheme

$$y^{\ell+1} = \left[\prod_{k=1}^{n}\left(I - \frac{\tau}{2}A_k\right)^{-1}\left(I + \frac{\tau}{2}A_k\right)\right]\left(y^\ell + \frac{\tau}{2}g^\ell\right) + \frac{\tau}{2}g^{\ell+1},\ \ell = 0, 1, 2, \ldots \tag{2.6}$$

Solutions of the above nonlinear system are traditionally computed via either a Newton-alike iterative procedure, or a linearization of $g^{\ell+1}$. In our approach, we prefer to replace the unknown $y^{\ell+1}$ in the source function by a suitable approximation, such as that obtained by using an Euler or extrapolation method [1, 8, 17].

*Remark* 2.1. Implementations with other boundary conditions, such as Neumann, Robin, or nonlocal conditions, may result in different coefficient matrices in (2.5) and (2.6). This will affect subsequent investigations of the stability, though similar results are expected. We shall leave detailed discussions to forthcoming papers.

*Remark* 2.2. Since the overall accuracy of eikonal transformation based exponential splitting used is of second order, the use if the [1/1] Padé approximation is sufficient [9]. However, different explicit or implicit methods due to other second order rational approximants for $S$ may also be constructed.

## 3. Analysis of the Asymptotic Stability

The concept of asymptotic stability has been extensively studied in numerous recent publications targeting at highly oscillatory wave applications. In the case, asymptotic profiles of targeted operators as the wavenumber, $\kappa$, tends to infinity are investigated while discretazation parameters $h$, $\tau$ remaining unchanged. For the latest development in the literature, the reader is referred to [3, 4, 5, 16, 18] and references therein. Let $\|\cdot\|_{2,h} = \sqrt{h}\|\cdot\|_2$ be the $h$-weighted spectral norm based on $\mathcal{D}_h$.

**Definition 3.1.** *Consider a semidiscretized scheme with a perturbation matrix $A$ for solving an oscillatory problem associated with a high wavenumber $\kappa \gg 1$. We say that the semidiscretized method is asymptotically stable if and only if there exist positive parameters $c$ and $d$ independent of $\kappa$ such that*

$$\|A\|_{2,h} \leq \frac{c}{\kappa^d} \quad \text{holds as} \quad \kappa \to \infty.$$

*The value of $d$ is called the asymptotical stability index of the underlying method.*

**Definition 3.2.** *Consider a fully discretized finite difference method with an amplification matrix $B$ for solving an oscillatory problem associated with a high wavenumber $\kappa \gg 1$. We say that the fully discretized method is asymptotically stable if and only if there exist positive parameters $c$ and $d$ independent of $\kappa$ such that*

$$\|B\|_{2,h} \leq \sqrt{h} + \frac{c}{\kappa^d} \quad \text{holds for} \quad \kappa \to \infty.$$

*The value of $d$ is called the asymptotical stability index of the numerical method.*

**Theorem 3.1.** *The eikonal transformation based and oscillation-free semidiscretized scheme* (2.5) *for solving* (2.1) *together with* (2.3), (2.4) *is unconditionally asymptotically stable with an index one.*

*Proof.* Consider the perturbation matrix $A = \sum_{k=1}^{n} A_k$. Then for any fixed $n,\ h$ we have

$$\begin{aligned}
\|A\|_{2,h} &\le \sum_{k=1}^{n} \|A_k\|_{2,h} \\
&\le \frac{1}{h^{3/2}} \sum_{k=1}^{n} \Big\| \Big( \overbrace{I_{2m} \otimes \cdots \otimes I_{2m}}^{n-k} \Big) \otimes T \otimes I_2 \otimes \Big( \overbrace{I_{2m} \otimes \cdots \otimes I_{2m}}^{k-1} \Big) \Big\|_2 \|D\|_2 \\
&= \frac{1}{h^{3/2}} \sum_{k=1}^{n} \|T\|_2 \|D\|_2 \ \le\ \frac{2n}{h^{3/2}\kappa} \ =\ \frac{c}{\kappa},
\end{aligned}$$

where $c = 2nh^{-3/2}$. Thus the theorem is true. $\square$

**Theorem 3.2.** *The semidiscretized formula based trapezoidal scheme* (1.4) *for solving* (2.1) *together with* (2.3), (2.4) *is unconditionally asymptotically stable with an index one.*

*Proof.* Recall (1.4). For any fixed $n,\ h$, let $c = \kappa_1 = \frac{4n\tau}{h^{3/2}}$. Then the $h$-weighted spectral norm of the amplification matrix, under the assumption $\kappa > \kappa_1$ and the fact that $\exp(x) \le \frac{1}{1-x},\ \forall\ 0 < x < 1$,

$$\begin{aligned}
\left\| \exp\left\{ \tau \sum_{k=1}^{n} A_k \right\} \right\|_{2,h} &\le \sqrt{h} \exp\left\{ \tau \sum_{k=1}^{n} \|A_k\|_2 \right\} \ \le \sqrt{h} \exp\left\{ \frac{\tau}{h^2} \sum_{k=1}^{n} \|T\|_2 \|D\|_2 \right\} \\
&\le \sqrt{h} \exp\left\{ \frac{2n\tau}{\kappa h^2} \right\} \le \frac{\sqrt{h}}{1 - \frac{c}{2\kappa}} \ =\ \sqrt{h} + \frac{\frac{c}{2\kappa}}{1 - \frac{c}{2\kappa}} \le \sqrt{h} + \frac{c}{\kappa}.
\end{aligned}$$

This completes our proof. $\square$

As for the baseline splitting method (2.6), we have the amplification matrix

$$B = \prod_{k=1}^{n} B_k = \prod_{k=1}^{n} \left( I - \frac{\tau}{2} A_k \right)^{-1} \left( I + \frac{\tau}{2} A_k \right), \quad \kappa > \kappa_1 \gg 1,$$

where $B_k = \left( I - \frac{\tau}{2} A_k \right)^{-1} \left( I + \frac{\tau}{2} A_k \right)$, and $A_p,\ A_q,\ 1 \le p, q \le n$, do not, in general, commute.

**Theorem 3.3.** *Let $\kappa \geq \kappa_1 = 2\tau/h^2$. Then the eikonal transformation based and oscillation-free baseline exponential splitting method* (2.6) *for solving* (2.1) *together with* (2.3), (2.4) *is unconditionally asymptotically stable with an index one.*

*Proof.* Since

$$B_k = I + \tau A_k \left(I - \frac{\tau}{2}A_k\right)^{-1},$$

it follows that

$$\begin{aligned}
\|B_k\|_{2,h} &= \left\|I + \tau A_k \left(I - \frac{\tau}{2}A_k\right)^{-1}\right\|_{2,h} \leq \sqrt{h} + \tau\sqrt{h}\,\|A_k\|_2 \left\|\left(I - \frac{\tau}{2}A_k\right)^{-1}\right\|_2 \\
&\leq \sqrt{h}\left(1 + \frac{\tau}{h^2}\|T\|_2\|D\|_2 \left\|\left(I - \frac{\tau}{2}A_k\right)^{-1}\right\|_2\right) \\
&\leq \sqrt{h}\left(1 + \frac{2\tau}{\kappa h^2} \left\|\left(I - \frac{\tau}{2}A_k\right)^{-1}\right\|_2\right). \qquad (3.1)
\end{aligned}$$

On the other hand, we observe that

$$\left(I - \frac{\tau}{2}A_k\right)^{-1} = I + \frac{\tau}{2}A_k\left(I - \frac{\tau}{2}A_k\right)^{-1}.$$

Thus,

$$0 < \left(1 - \frac{\tau}{h^2\kappa}\right)\left\|\left(I - \frac{\tau}{2}A_k\right)^{-1}\right\|_2 \leq \left(1 - \frac{\tau}{2}\|A_k\|_2\right)\left\|\left(I - \frac{\tau}{2}A_k\right)^{-1}\right\|_2 \leq 1.$$

It follows that

$$\left\|\left(I - \frac{\tau}{2}A_k\right)^{-1}\right\|_2 \leq \frac{h^2\kappa}{h^2\kappa - \tau} \leq 2$$

due to the fact that $\theta(x) = x(x-\tau)^{-1} \leq \theta(2\tau)$ for any $x \geq 2\tau$. Recall (3.1),

$$\|B_k\|_{2,h} \leq \sqrt{h}\left(1 + \frac{4\tau}{\kappa h^2}\right).$$

Consequently,

$$\|B\|_{2,h} \leq \sqrt{h}\left(1 + \frac{4\tau}{\kappa h^2}\right)^n = \sqrt{h} + \frac{c}{\kappa},$$

where

$$c = \frac{4\tau}{h^{3/2}}\left(n + \frac{n(n-1)}{2!}\xi + \frac{n(n-1)(n-2)}{3!}\xi^2 + \cdots + \xi^{n-1}\right), \ \xi = \frac{4\tau}{\kappa_1 h^2}$$

due to the binomial expansion formula. Therefore the splitting method is unconditionally asymptotically stable with the index $d = 1$. $\square$

The above investigation implies

**Corollary 3.1.** *Let $\kappa_1 \geq 2\tau/h^2$. Then the eikonal transformation based and oscillation-free sequential splitting method* (1.6), *parallel splitting method* (1.7) *and combined splitting method* (1.8) *for solving* (2.1) *together with* (2.3), (2.4) *are unconditionally asymptotically stable with an index one.*

*Remark* 3.1. Theorems 3.1–3.3 and Corollary 3.1 ensure that the asymptotical stability index of the numerical methods involved is one. However there is a possibility to improve this result, in particular when improved second order exponential splitting or certain high order formulas [2] are involved. However, the tasks can be technically challenging.

*Remark* 3.2. The grid size $h$ can be different in different transverse directions. This may or may not affect dimensions of the matrix operators resulted [11]. However, discussions in the former situation are apparently more complicated. Nevertheless, stability analysis via a variable $h$-weighted norm can be challenging. But different matrix norms can also be utilized. We shall again leave these issues to our forthcoming discussions.

## 4. A Simulation Example

As an illustration of the efficiency and capability of the splitting schemes studied, oriented from (2.1), we consider a two-dimensional paraxial Helmholtz equation,

$$2\mathbf{i}\kappa E_z = E_{x_1x_1} + E_{x_2x_2} - \kappa^2 E, \quad (x_1, x_2) \in \mathcal{D},\ z > z_0,$$

where $\mathcal{D} = \{(x_1, x_2) : \ -a < x_1, x_2 < a\}$, $a \in \mathbb{R}$. Due to its constant cross section index profile, the above equation can be reformulated to the following [6],

$$E_z = \gamma E_{x_1x_1} + \gamma E_{x_2x_2}, \quad (x_1, x_2) \in \mathcal{D},\ z > z_0 > 0, \tag{4.1}$$

where $\gamma = -\mathbf{i}/(2\kappa)$. Further, consider the Gaussian beam initial function,

$$E(x_1, x_2, z) = \frac{\exp\{-(x_1^2 + x_2^2)/[2(1 + \mathbf{i}z_{11})]\}}{1 + \mathbf{i}z_{11}}, \quad (x_1, x_2) \in \mathcal{D},\ z > z_0 > 0, \tag{4.2}$$

where $z_{11} > 0$. Equations (4.1), (4.2) models a variety of highly oscillatory wave focusing exactly at $z_{11}$ [11]. Any reliable numerical method for solving the problem must be asymptotically stabile and reproduce correctly the underlying focusing phenomenon [11, 15, 18]. This has become an effective testing stone for the correctness and accuracy of highly oscillatory wave simulations. Targeting at the numerical solution of (4.1), (4.2) together with homogeneous first boundary conditions (2.3), we test both the ADI oriented sequential splitting formula (1.6) as well as LOD oriented parallel splitting formula (1.7) for the eikonal transformation based system (2.5) in experiments. Since numerical solutions obtained are similar, for the sake of simplicity in presentations, herewith we only show results of the sequential splitting with $h = 1/300$, and dimensional Courant numbers $15/2, 75/2$ when $z_{11} = 50, 100$, respectively.

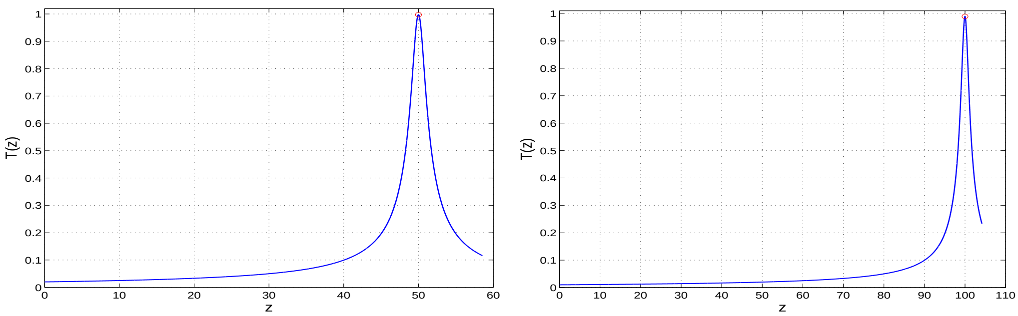


FIGURE 4.1. Trajectories of maximal modules function $T(z)$ as $z$ increases till focusing regions (LEFT: $z_{11} = 50$, RIGHT: $z_{11} = 100$). Little differences between solutions of (1.6) and (1.7) are found.

First, trajectories of the modules function $T(z) = \max\limits_{(x_1,x_2)} |E(x_1, x_2, z)|$ as $z$ travels from $z_0$ to focusing regions are shown in Figure 4.1. We may observe that the energy grows monotonically till the focusing point in cases when $\kappa = 50,\ 100$. Peak values of $E$, $\max\limits_{z} T_{z_{11}=50}(z) = 0.99747361$ and $\max\limits_{z} T_{z_{11}=100}(z) = 0.98958524$, are highlighted respectively. The simulations match precisely measurements from laboratorial experiments [11, 18].

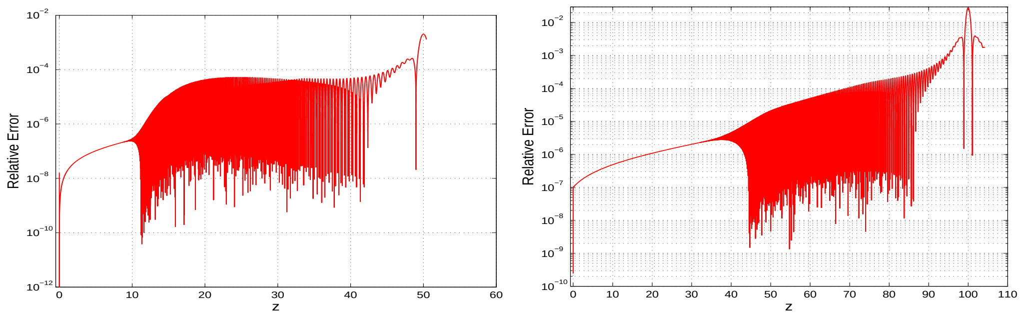


FIGURE 4.2. Relative posteriori errors of the approximation $T(z)$ as $z$ increases till focusing regions (LEFT: $z_{11} = 50$, RIGHT: $z_{11} = 100$). A logarithmic scale is used in the $y$-direction to shown more details of the delicate computational error dynamics.

Next, in Figure 4.2, we plot corresponding relative posteriori errors $\mathcal{E}_{z_{11}=50}(z)$ and $\mathcal{E}_{z_{11}=100}(z)$, where

$$\mathcal{E}_{z_{11}}(z) = \frac{\left|T_{z_{11},\tau}(z) - T_{z_{11},\tau/2^m}(z)\right|}{|T_{z_{11},\tau}(z)|}, \quad 0 < z < z_{11}.$$

Parametric values $m = 1, 2$ are utilized in cases of $z_{11} = 50, 100$, respectively. It is interesting to see in Figure 4.2 that the posteriori errors are well below $10^{-2}\%$ throughout beam propagations. They reach maximums, $\max_z \mathcal{E}_{z_{11}=50}(z) = 0.00202885$ and $\max_z \mathcal{E}_{z_{11}=100}(z) = 0.02815409$ only at respective focusing points (this can be a good indicator that suitable grid refinements [1, 6] may be introduced to focusing regions). Nevertheless, the overall error performances are highly satisfactory.

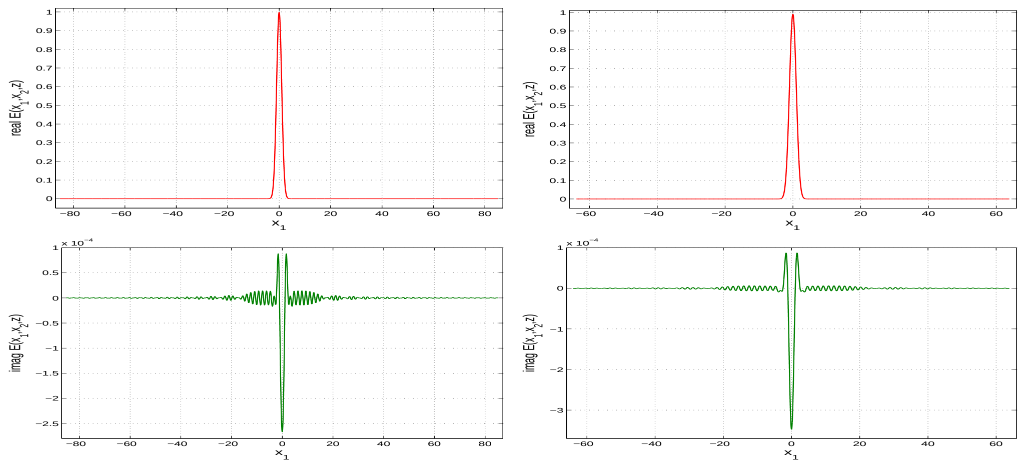

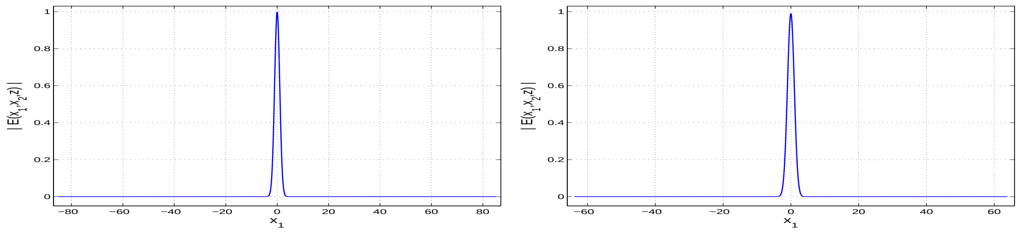


FIGURE 4.3. Focusing numerical solution $E$ (LEFT: $z_{11} = 50$, RIGHT: $z_{11} = 100$). From top to bottom are real, imaginary parts and modules of the solution, respectively.

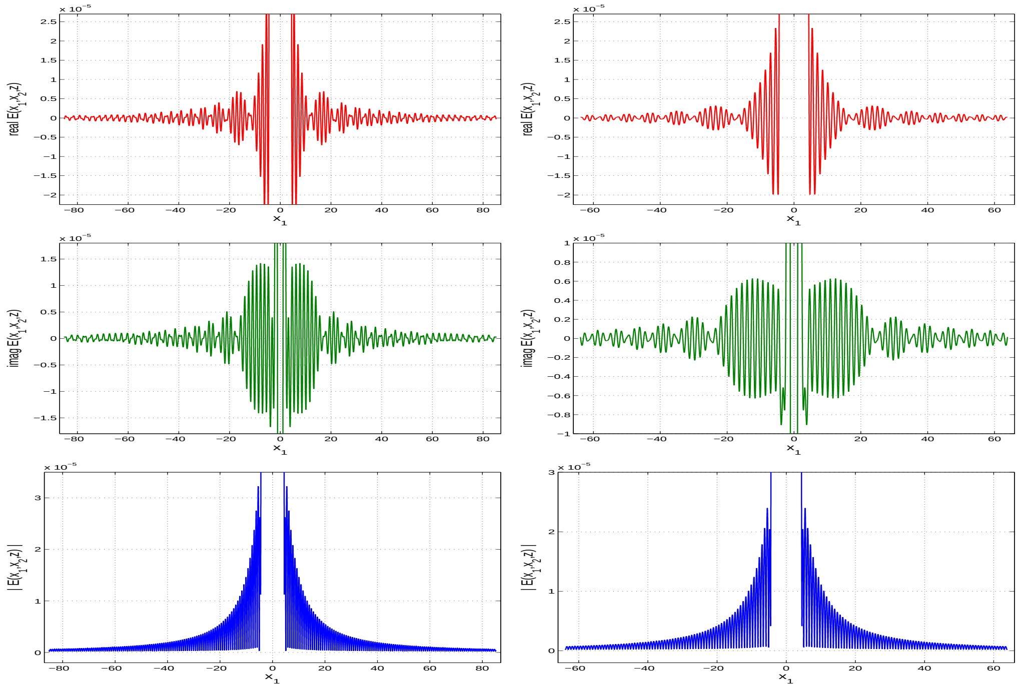


FIGURE 4.4. Enlarged focusing numerical solution details (LEFT: $z_{11} = 50$, RIGHT: $z_{11} = 100$). From top to bottom are real, imaginary parts and modules of the solution, respectively.

Further, in Figure 4.3, we show simulated focusing solution profiles in the transverse direction $x_1$ since those in the $x_2$-direction are similar. Again, little differences between solutions of (1.6) and (1.7) are found. The solutions blow-up within a narrow transverse region. This indicates high energy concentrations as expected. The profiles well agree with known computational results documented in [11, 16, 18]. To see more details of the oscillation nature of propagating waves, we locally enlarge images in Figure 4.3 to that in Figure 4.4. Though amplitudes of perturbations are relatively small as compared with focusing peaks, wave oscillations are still persistent and clearly visible throughout simulation experiments. The phenomenon well agrees with explorations of errors in linearized and localized wave approximations [15, 17].

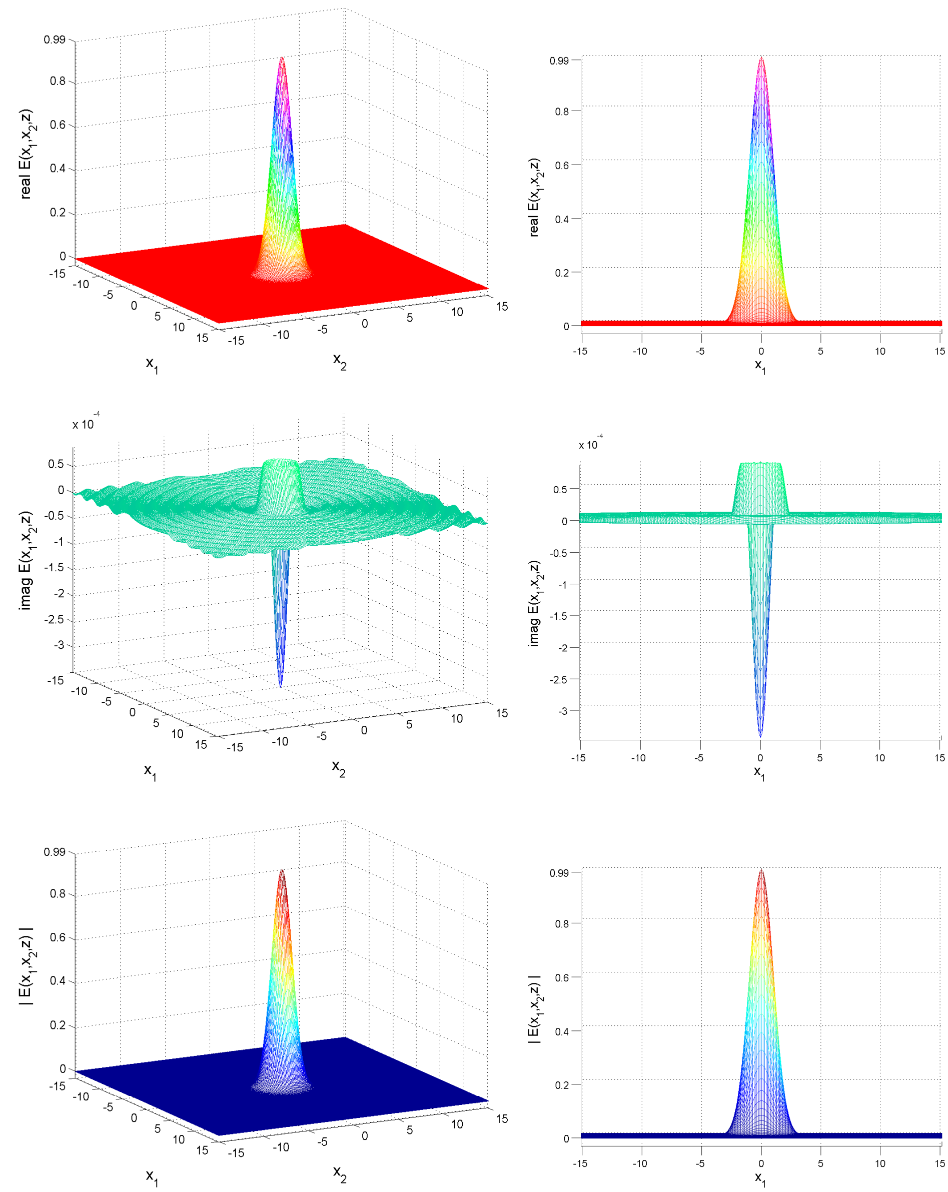


FIGURE 4.5. 3D views of the focusing numerical solution $E$ (RIGHT: $x_1$-direction projections; $z_{11} = 100$). From top to bottom are real, imaginary parts and modules of the solution, respectively.

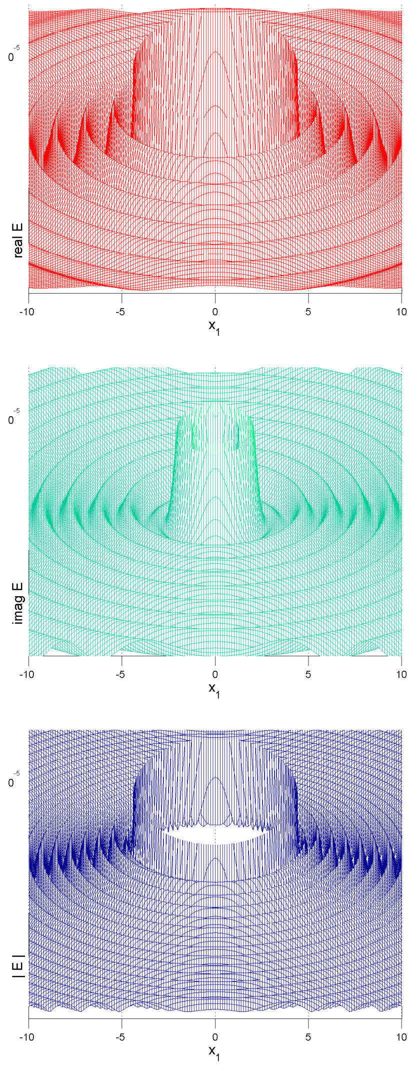


FIGURE 4.6. 3D views of the enlarged focusing numerical solution ($z_{11} = 100$). The $E$-range used is $\left[-0.3 \times 10^{-4}, 0.3 \times 10^{-4}\right]$. From top to bottom are real, imaginary parts and modules of the solution, respectively.

Finally, Figures 4.5 and 4.6 are devoted to 3-dimensional views of the focusing numerical solution via the splitting methods (1.6) and (1.7). The solution surfaces are highly vital. They provide precise information about an ideal focusing when a large value of $z_{11} = 100$ is applied. The simulations are important to various applications including massive and composite micro lens design and production [6]. In the locally enlarged figures in Figure

4.6, circular highly oscillatory waves are clearly visible. There has been no surprise that numerical solutions from asymptotically stable sequential and parallel splitting computations exhibit satisfactory results. Again, transverse step $h = 1/300$ and dimensional Courant number $\tau/h^2 = 75/2$ are used in Figures 4.5 and 4.6 simulations.

## 5. Conclusions

This paper explores an inherent relevance between the standard first order exponential splitting algorithm (1.5) and second order sequential, parallel and combined splitting formulas (1.6)–(1.8). Based on this, an eikonal transformation based exponential splitting method for solving the highly oscillatory $n$-dimensional paraxial Helmholtz equation is investigated. Key asymptotic stability of the numerical scheme is proven. It is found that the asymptotical stability index of the underlying method is one.

The asymptotic stability studied in this paper can also be extended for examining similar oscillation-free algorithms, especially those for solving more sophisticated and Gaussian beam oriented problems including high dimensional Kukhtarev systems in photorefractive wave and wave-material interaction applications [11, 15], or Maxwell's equations in universal electromagnetic fields and cosmology [5, 7, 19]. Although most discussions presented in this paper involve only homogeneous first boundary conditions and on uniform transverse grids, reflective or nonlocal conditions together with grid adaptations [1, 6] can also be incorporated. In addition, certain target-oriented splitting strategies, such as the asymptotic and high order splitting [2, 12, 13], may also be employed for higher order multi-dimensional wave approximations. The study of the nonlinear numerical stability with eikonal formulas for highly oscillatory waves, however, are still in its infancy in general. These are, needless to say, among our continuing endeavors.

## 6. Appendix

We show that (1.6)–(1.8) are indeed second order exponential splitting (see definitions in [9] §4.1 and [12]). To this end, we need

**Lemma 6.1.** *Let $A,\ B \in \mathbb{C}^{m\times m}$, $m \geq 1$, and $A,\ B$ be independent of $\tau > 0$. Then* $[\exp(\tau A), \exp(\tau B)] \equiv \exp(\tau A)\exp(\tau B) - \exp(\tau B)\exp(\tau A) = \tau^2[A,B] + \mathcal{O}(\tau^3)$ *as* $\tau \to 0^+$.

*Proof.* Expanding matrix exponentials in the commutator we acquire that

$$\begin{aligned}
&\exp(\tau A)\exp(\tau B) - \exp(\tau B)\exp(\tau A)\\
&\quad= \left(I + \tau A + \frac{\tau^2}{2}A^2 + \frac{\tau^3}{3!}A^3 + \cdots\right)\left(I + \tau B + \frac{\tau^2}{2}B^2 + \frac{\tau^3}{3!}B^3 + \cdots\right)\\
&\qquad - \left(I + \tau B + \frac{\tau^2}{2}B^2 + \frac{\tau^3}{3!}B^3 + \cdots\right)\left(I + \tau A + \frac{\tau^2}{2}A^2 + \frac{\tau^3}{3!}A^3 + \cdots\right)\\
&\quad= I + \tau B + \frac{\tau^2}{2}B^2 + \frac{\tau^3}{3!}B^3 + \tau A + \tau^2 AB + \frac{\tau^3}{2}AB^2\\
&\qquad + \frac{\tau^2}{2}A^2 + \frac{\tau^3}{2}A^2B + \frac{\tau^3}{3!}A^3 - I - \tau A - \frac{\tau^2}{2}A^2 - \frac{\tau^3}{3!}A^3\\
&\qquad - \tau B - \tau^2 BA - \frac{\tau^3}{2}BA^2 - \frac{\tau^2}{2}B^2 - \frac{\tau^3}{2}B^2A - \frac{\tau^3}{3!}B^3 + \cdots\\
&\quad= \tau^2(AB - BA) + \frac{\tau^3}{2}\left(AB^2 + A^2B - BA^2 - B^2A\right) + \mathcal{O}(\tau^4)\\
&\quad= \tau^2[A,B] + \mathcal{O}(\tau^3), \quad \tau \to 0^+.
\end{aligned}$$

This ensures our lemma. □

We first show that

$$P_K(\tau) = S(A_1, A_2, \ldots, A_K, \tau/2)S(A_K, A_{K-1}, \ldots, A_1, \tau/2), \quad 0 < \tau \ll 1,$$

is a second order exponential splitting for $K \geq 2$. Note that

$$P_2(\tau) = \exp\left(\frac{\tau}{2}A_1\right)\exp(\tau A_2)\exp\left(\frac{\tau}{2}A_1\right) = \exp(\tau(A_1 + A_2)) + \mathcal{O}(\tau^3)$$

is the standard second order Strang's splitting [9, 12]. Let $K = 3$. We have

$$\begin{aligned}
&\exp\left(\tau(A_1 + A_2 + A_3)\right) = \exp\left(\frac{\tau}{2}A_1\right)\exp\left(\tau(A_2 + A_3)\right)\exp\left(\frac{\tau}{2}A_1\right) + \mathcal{O}(\tau^3)\\
&\quad= \exp\left(\frac{\tau}{2}A_1\right)\left\{\exp\left(\frac{\tau}{2}A_2\right)\exp(\tau A_3)\exp\left(\frac{\tau}{2}A_2\right) + \mathcal{O}(\tau^3)\right\}\exp\left(\frac{\tau}{2}A_1\right) + \mathcal{O}(\tau^3)\\
&\quad= \exp\left(\frac{\tau}{2}A_1\right)\exp\left(\frac{\tau}{2}A_2\right)\exp(\tau A_3)\exp\left(\frac{\tau}{2}A_2\right)\exp\left(\frac{\tau}{2}A_1\right) + \mathcal{O}(\tau^3)\\
&\quad= S(A_1, A_2, A_3\tau/2)S(A_3, A_2, A_1, \tau/2) + \mathcal{O}(\tau^3) = P_3(\tau) + \mathcal{O}(\tau^3).
\end{aligned}$$

Assume that $\exp\left(\tau(A_1 + A_2 + \cdots + A_n)\right) = P_n(\tau) + \mathcal{O}(\tau^3),\ n > 3$. Now,

$$
\begin{aligned}
\exp\left(\tau(A_1 + A_2 + \cdots + A_n + A_{n+1})\right) &= \exp\left(\frac{\tau}{2}A_1\right)\exp\left(\frac{\tau}{2}A_2\right)\cdots \\
&\quad \times \cdots \exp\left(\frac{\tau}{2}A_{n-1}\right)\exp(\tau(A_n + A_{n+1}))\exp\left(\frac{\tau}{2}A_{n-1}\right)\cdots \\
&\quad \times \cdots \exp\left(\frac{\tau}{2}A_2\right)\exp\left(\frac{\tau}{2}A_1\right) + \mathcal{O}(\tau^3) \\
&= \exp\left(\frac{\tau}{2}A_1\right)\exp\left(\frac{\tau}{2}A_2\right)\cdots\exp\left(\frac{\tau}{2}A_{n-1}\right) \\
&\quad \times \left\{\exp\left(\frac{\tau}{2}A_n\right)\exp\left(\tau A_{n+1}\right)\exp\left(\frac{\tau}{2}A_n\right) + \mathcal{O}(\tau^3)\right\} \\
&\quad \times \exp\left(\frac{\tau}{2}A_{n-1}\right)\cdots\exp\left(\frac{\tau}{2}A_2\right)\exp\left(\frac{\tau}{2}A_1\right) + \mathcal{O}(\tau^3) \\
&= \exp\left(\frac{\tau}{2}A_1\right)\exp\left(\frac{\tau}{2}A_2\right)\cdots\exp\left(\frac{\tau}{2}A_{n-1}\right)\exp\left(\frac{\tau}{2}A_n\right)\exp(\tau A_{n+1}) \\
&\quad \times \exp\left(\frac{\tau}{2}A_n\right)\exp\left(\frac{\tau}{2}A_{n-1}\right)\cdots\exp\left(\frac{\tau}{2}A_2\right)\exp\left(\frac{\tau}{2}A_1\right) + \mathcal{O}(\tau^3) \\
&= S(A_1, A_2, \ldots, A_n, A_{n+1}\tau/2)S(A_{n+1}, A_n, \ldots, A_1, \tau/2) + \mathcal{O}(\tau^3) \\
&= P_{n+1}(\tau) + \mathcal{O}(\tau^3), \quad \tau \to 0^+.
\end{aligned}
$$

Therefore $P_K(\tau)$ must be a second order exponential splitting according to the induction used.

Next, we denote

$$
Q_K(\tau) = \frac{1}{2}\left\{S(A_1, A_2, \ldots, A_K, \tau) + S(A_K, A_{K-1}, \ldots, A_1, \tau)\right\}, \quad 0 < \tau \ll 1,
$$

where $K \geq 2$. Apparently,

$$
Q_2(\tau) = \frac{1}{2}\left\{S(A_1, A_2, \tau) + S(A_2, A_1, \tau)\right\} = \exp(\tau(A_1 + A_2)) + \mathcal{O}(\tau^3)
$$

is the conventional second order parallel splitting [12, 14]. Further,

$$
\begin{aligned}
&\exp(\tau(A_1 + A_2 + A_3)) \\
&= \frac{1}{2}\{\exp(\tau A_1)\exp(\tau(A_2 + A_3)) + \exp(\tau(A_3 + A_2))\exp(\tau A_1)\} + \mathcal{O}(\tau^3) \\
&= \frac{1}{4}\exp(\tau A_1)\left\{\exp(\tau A_2)\exp(\tau A_3) + \exp(\tau A_3)\exp(\tau A_2) + \mathcal{O}(\tau^3)\right\} \\
&\ + \frac{1}{4}\left\{\exp(\tau A_2)\exp(\tau A_3) + \exp(\tau A_3)\exp(\tau A_2) + \mathcal{O}(\tau^3)\right\}\exp(\tau A_1) + \mathcal{O}(\tau^3) \\
&= \frac{1}{2}\{\exp(\tau A_1)\exp(\tau A_2)\exp(\tau A_3) + \exp(\tau A_3)\exp(\tau A_2)\exp(\tau A_1)\} \\
&\ + \frac{1}{4}\exp(\tau A_1)\{\exp(\tau A_3)\exp(\tau A_2) - \exp(\tau A_2)\exp(\tau A_3)\} \\
&\ + \frac{1}{4}\{\exp(\tau A_2)\exp(\tau A_3) - \exp(\tau A_3)\exp(\tau A_2)\}\exp(\tau A_1) + \mathcal{O}(\tau^3) \\
&= Q_3(\tau) + \frac{1}{4}\Big\{ \exp(\tau A_1)\,[\exp(\tau A_3), \exp(\tau A_2)] \\
&\ - [\exp(\tau A_3), \exp(\tau A_2)]\exp(\tau A_1)\Big\} + \mathcal{O}(\tau^3) \\
&= Q_3(\tau) + \frac{1}{4}\left\{\left(I + \tau A_1 + \frac{\tau^2}{2}A_1^2 + \cdots\right)\left(\tau^2[A_3, A_2] + \mathcal{O}(\tau^2)\right)\right. \\
&\ \left. - \left(\tau^2[A_3, A_2] + \mathcal{O}(\tau^2)\right)\left(I + \tau A_1 + \frac{\tau^2}{2}A_1^2 + \cdots\right)\right\} + \mathcal{O}(\tau^3) \\
&= Q_3(\tau) + \frac{1}{4}\left\{\tau^2[A_3, A_2] - \tau^2[A_3, A_2] + \mathcal{O}(\tau^3)\right\} + \mathcal{O}(\tau^3) \\
&= Q_3(\tau) + \mathcal{O}(\tau^3).
\end{aligned}
$$

Therefore $Q_3(\tau)$ is of second order. Assume the same to be true for $Q_n(\tau),\ n > 3$. Then,

$$
\begin{aligned}
&\exp\left(\tau(A_1 + A_2 + \cdots + A_n + A_{n+1})\right) \\
&= \frac{1}{2}\left\{\exp(\tau A_1)\exp(\tau A_2)\cdots\exp(\tau A_{n-1})\exp(\tau(A_n + A_{n+1}))\right. \\
&\left. + \exp(\tau(A_{n+1} + A_n))\exp(\tau A_{n-1})\cdots\exp(\tau A_2)\exp(\tau A_1)\right\} + \mathcal{O}(\tau^3) \\
&= \frac{1}{4}\exp(\tau A_1)\exp(\tau A_2)\cdots\exp(\tau A_{n-1}) \\
&\times \{\exp(\tau A_n)\exp(\tau A_{n+1}) + \exp(\tau A_{n+1})\exp(\tau A_n)\} \\
&+ \frac{1}{4}\{\exp(\tau A_n)\exp(\tau A_{n+1}) + \exp(\tau A_{n+1})\exp(\tau A_n)\} \\
&\times \exp(\tau A_{n-1})\cdots\exp(\tau A_2)\exp(\tau A_1)] + \mathcal{O}(\tau^3) \\
&= \frac{1}{4}\exp(\tau A_1)\exp(\tau A_2)\cdots\exp(\tau A_{n-1})\exp(\tau A_n)\exp(\tau A_{n+1}) \\
&+ \frac{1}{4}\exp(\tau A_1)\exp(\tau A_2)\cdots\exp(\tau A_{n-1})\exp(\tau A_{n+1})\exp(\tau A_n) \\
&+ \frac{1}{4}\exp(\tau A_{n+1})\exp(\tau A_n)\exp(\tau A_{n-1})\cdots\exp(\tau A_2)\exp(\tau A_1) \\
&+ \frac{1}{4}\exp(\tau A_n)\exp(\tau A_{n+1})\exp(\tau A_{n-1})\cdots\exp(\tau A_2)\exp(\tau A_1) + \mathcal{O}(\tau^3) \\
&= Q_{n+1}(\tau) + \frac{1}{4}\exp(\tau A_1)\exp(\tau A_2)\cdots\exp(\tau A_{n-1})[\exp(\tau A_{n+1}), \exp(\tau A_n)] \\
&- \frac{1}{4}[\exp(\tau A_{n+1}), \exp(\tau A_n)]\exp(\tau A_{n-1})\cdots\exp(\tau A_2)\exp(\tau A_1) + \mathcal{O}(\tau^3).
\end{aligned}
$$

Since

$$
\begin{aligned}
&\exp(\tau A_1)\exp(\tau A_2)\cdots\exp(\tau A_{n-1}) = \left(I + \tau A_1 + \frac{\tau^2}{2}A_1^2 + \cdots\right) \\
&\quad\times\left(I + \tau A_2 + \frac{\tau^2}{2}A_2^2 + \cdots\right)\cdots\left(I + \tau A_{n-1} + \frac{\tau^2}{2}A_{n-1}^2 + \cdots\right) \\
&\quad= I + \tau(A_1 + A_2 + \cdots A_{n-1}) + \mathcal{O}(\tau^2), \\
&\exp(\tau A_{n-1})\cdots\exp(\tau A_2)\exp(\tau A_1) = \left(I + \tau A_{n-1} + \frac{\tau^2}{2}A_{n-1}^2 + \cdots\right) \\
&\quad\times\left(I + \tau A_{n-2} + \frac{\tau^2}{2}A_{n-2}^2 + \cdots\right)\cdots\left(I + \tau A_1 + \frac{\tau^2}{2}A_1^2 + \cdots\right) \\
&\quad= I + \tau(A_1 + A_2 + \cdots A_{n-1}) + \mathcal{O}(\tau^2)
\end{aligned}
$$

and $[\exp(\tau A_{n+1}), \exp(\tau A_n)] = \tau^2[A_{n+1}, A_n] + \mathcal{O}(\tau^3)$ according to Lemma 6.1, we have

$$\exp\left(\tau(A_1 + A_2 + \cdots + A_n + A_{n+1})\right) = Q_{n+1}(\tau) + \mathcal{O}(\tau^3), \quad \tau \to 0^+.$$

The above indicates that $Q_{n+1}(\tau)$ is a second order formula. Therefore (1.6)–(1.8) are second order exponential splitting.

### 7. Acknowledgements

The authors would like to thank the anonymous referees for their valuable comments and suggestions that enhanced the quality and presentation of this paper. The second author also appreciates the support and encouragements from the Science and Technology Development Fund and the University of Macau, Macao, China.

## References

[1] M. A. Beauregard and Q. Sheng, An adaptive splitting approach for the quenching solution of reaction-diffusion equations over nonuniform grids, J. Comptat. Appl. Math., 241 (2013), 30–44.

[2] S. Blanes, F. Casas, P. Chartier and A. Murua, Optimized high-order splitting methods for some classes of parabolic equations, Math. Comput., 82 (2013), 1559–1576.

[3] H. Brunner, A. Iserles and S. P. Nørsett, The spectral problem for a class of highly oscillatory Fredholm differential equations, IMA J. Numer. Anal., 30 (2010), 108–130.

[4] M. Condon, A. Deaño and A. Iserles, On highly oscillatory problems arising in electronic engineering, Math. Model. Numer. Anal., 43 (2009), 785–804.

[5] B. Engquist, A. Fokas, E. Hairer and A. Iserles, Highly Oscillatory Problems, London Math. Soc., London, 2009.

[6] L. Gonzalez, S. Guha, J. W. Rogers and Q. Sheng, An effective $z$-stretching method for paraxial light beam propagation simulations, J. Comput. Phys., 227 (2008), 7264–7278.

[7] P. Horava and C. M. Melby-Thompson, General covariance in quantum gravity at a Lifshitz point, Phys. Rev. D, 82 (2010), 64027-64040.

[8] Ch Lubich, I. H. Sloan and V. Thom'ee, Nonsmooth data error estimates for approximations of an evolution equation with a positive type memory term, Math. Comput., 65 (1996), 1–17.

[9] R. I. McLachlan and G. R. W. Quispel, Splitting methods, Acta Numerica, 11 (2002), 341–434.

[10] H.-G. Roos and M. Schopf, Convergence and stability in balanced norms of finite element methods on Shishkin meshes for reaction-diffusion problems, Z. angew. Math. Mech., (2014), doi: 10.1002/zamm.201300226.

[11] B. E. A. Saleh and M. C. Teich, Fundamentals of Photonics, John Wiley & Sons, New York, 1991.

[12] Q. Sheng, Solving linear partial differential equations by exponential splitting, *IMA J. Numer. Anal.,* 9 (1989), 199–212.

[13] Q. Sheng, A note on asymptotic splitting and its applications, Math. Comput. Modelling, 20 (1994), 45–58.

[14] Q. Sheng, ADI Methods, Encyclopedia of Applied and Computational Mathematics, Springer-Verlag, Berlin and Heidelberg, in press, 2015.

[15] Q. Sheng, S. Guha and L. Gonzalez, An exponential transformation based splitting method for fast computations of highly oscillatory solutions, J. Comput. Appl. Math., 235 (2011), 4452–4463.

[16] Q. Sheng and H. Sun, On the stability of an oscillation-free ADI method for highly oscillatory wave equations, Comm. Comput. Phys, 12 (2012), 1275–1292.

[17] E. H. Twizell, Y. Wang and W. G. Price, Chaos-free numerical solutions of reaction-diffusion equations, Proc. Roy. Soc. London Sect. A, 430 (1991), 541–576.

[18] N. P. van der Aa, The Rigorous Coupled-Wave Analysis, Ph.D. dissertation, Faculteit Wiskunde & Informatica, Technische Universiteit Eindhoven, the Netherland, 2007.

[19] T. Zhu, A. Wang, G. Cleaver, K. Kirsten and Q. Sheng, Infationary cosmology with nonlinear dispersion relations, Phys. Rev. D., 89 (2014) 043507:1-23.